Re-examining the $X(4630)$ resonance in the reaction $e^+e^- \to \Lambda_c^+ \bar{\Lambda}_c^-$

Ling-Yun Dai,[1,*] Johann Haidenbauer,[1,†] and Ulf-G. Meißner[2,1,‡]

[1]*Institut für Kernphysik, Institute for Advanced Simulation and Jülich Center for Hadron Physics,
Forschungszentrum Jülich, D-52425 Jülich, Germany*
[2]*Helmholtz Institut für Strahlen- und Kernphysik and Bethe Center for Theoretical Physics,
Universität Bonn, D-53115 Bonn, Germany*

The reaction $e^+e^- \to \Lambda_c^+ \bar{\Lambda}_c^-$ is investigated at energies close to the threshold with emphasis on the role played by the $X(4630)$ resonance. The interaction in the final $\Lambda_c^+ \bar{\Lambda}_c^-$ system, constructed within chiral effective field theory and supplemented by a pole diagram that represents a bare $X(4630)$ resonance, is taken into account rigorously. The pole parameters of the $X(4630)$ are extracted and found to be compatible with the ones of the $X(4660)$ resonance that have been established in the reaction $e^+e^- \to \pi^+\pi^-\psi(2S)$. The actual result for the $X(4630)$ is $M = (4652.5 \pm 3.4)$ MeV and $\Gamma = (62.6 \pm 5.6)$ MeV. Predictions for the Λ_c^+ electromagnetic form factors in the timelike region are presented.

I. INTRODUCTION

Over the last decade or so overwhelming experimental evidence has accumulated that casts some doubts on our understanding of the hadron spectrum so far. Specifically, at energies above the open charm production threshold a plethora of structures were seen in experiments which do not really fit into the standard picture that mesons are composed out of quark-antiquark pairs. For recent overviews and discussions of these structures, commonly referred to as X, Y, and Z states, see for example [1–3].

Among these structures is a state listed as $X(4660)$ in the latest compilation of the Particle Data Group (PDG) [4]. This $X(4660)$ [also known as $Y(4660)$] was seen in the reaction $e^+e^- \to \pi^+\pi^-\psi(2S)$ [5–7]. Additionally, a structure called the $X(4630)$ was seen in the reaction $e^+e^- \to \Lambda_c^+ \bar{\Lambda}_c^-$ [8] in a very nearby energy region. Finally, there is also an enhancement around 4660 MeV in the $\Lambda_c^+ \bar{\Lambda}_c^-$ invariant mass measured in the reaction $\bar{B} \to \Lambda_c^+ \bar{\Lambda}_c^- \bar{K}$ [9]. Since the mass and width derived from a Breit-Wigner based fit to the $e^+e^- \to \Lambda_c^+ \bar{\Lambda}_c^-$ data yielded results that are consistent with those deduced from the $\pi^+\pi^-\psi(2S)$ channel it was already conjectured in Ref. [8] that the states in question could be the same. The subsequent works by Bugg [10], Cotugno *et al.* [11], and Guo *et al.* [12] took up this interpretation and tried to corroborate it with arguments and also with explicit calculations. Indeed, the PDG adopted likewise this point of view by listing the states under the same heading [4]. Note, however, that the statement "the states are not necessarily the same" is added. An entirely different issue is the dynamical origin of the state(s). While some studies assign the $X(4660)$ to a regular $c\bar{c}$

charmonium state, for example to the $\psi(6S)$ [13], or interpret it as tetraquark state [11], others see in it a $f_0(980)\psi'$ bound state [14]. For yet another and may be somewhat unorthodox explanation see Ref. [15].

In the present work we focus on the question whether the $X(4660)$ and $X(4630)$ could be indeed one and the same state—and leave the issue of the dynamical origin aside. While the background in the reaction $e^+e^- \to \pi^+\pi^-\psi(2S)$ is fairly small and, therefore, one could argue that an extraction of the resonance parameters via a Breit-Wigner fit to the data [6,7] might be justified, this definitely cannot be said for $e^+e^- \to \Lambda_c^+ \bar{\Lambda}_c^-$. Due to the proximity of the $\Lambda_c^+ \bar{\Lambda}_c^-$ threshold (at 4573 MeV) there is a strong distortion of the signal and, clearly, the measured cross section does not resemble a typical Breit-Wigner shape at all [8]. Moreover, assuming that the transition is mediated by one-photon exchange the $\Lambda_c^+ \bar{\Lambda}_c^-$ will be either in the $^3S_1$ or $^3D_1$ partial wave. In the S wave strong effects from the final state interaction (FSI) are expected that will likewise influence the energy dependence of the cross section. Such FSI effect arise from the coupling to the resonance itself, but also from the residual interaction between the Λ_c^+ and $\bar{\Lambda}_c^-$, say due to possible t-channel meson exchange, on top of an s-channel resonance contribution.

The effects discussed above have been already considered in the arguments in Refs. [10,12] and are to some extent also simulated in the numerical results presented there. However, since close to threshold a rather delicate interplay between the resonance and the residual interaction (sometimes also called background or nonpole contribution) has to be expected we believe that a more rigorous treatment is required in order to obtain quantitatively reliable results and solid conclusions. In recent studies of the reactions $e^+e^- \to p\bar{p}$ [16] and $e^+e^- \to \Lambda\bar{\Lambda}$ [17] near their respective threshold we have set up a framework that allows one to implement the FSI effects from the

*[*]l.dai@fz-juelich.de
[†]j.haidenbauer@fz-juelich.de
[‡]meissner@hiskp.uni-bonn.de

116001-1

baryons in a microscopic way. This formalism can be applied straightforwardly to the $e^+e^- \to \Lambda_c^+\bar{\Lambda}_c^-$ case as will be demonstrated in the present paper. Though no resonances are present in the two reactions above, a clear enhancement in the corresponding near-threshold cross sections has been found in pertinent experiments. Our studies showed that a proper inclusion of the FSI effects within our formalism allows one to achieve an excellent description of the measured cross sections. In its application to $e^+e^- \to \Lambda_c^+\bar{\Lambda}_c^-$ essential features such as the interplay between the pole and nonpole part of the potential but also unitarity constraints on the $\Lambda_c^+\bar{\Lambda}_c^-$ amplitude are implemented. Moreover, a reliable extraction of the pole parameters of the $X(4630)$ resonance is possible, that does not rely on a Breit-Wigner parameterization, and these values can then be confronted with the resonance properties extracted from the $e^+e^- \to \pi^+\pi^-\psi(2S)$ data.

The paper is structured as follows: The ingredients of the $\Lambda_c^+\bar{\Lambda}_c^-$ potential that is employed for generating the FSI are summarized in Sec. II. The potential involves contact terms analogous to those that arise in chiral effective field theory (EFT) up to next-to-leading order (NLO) and a contribution from a (bare) resonance. In addition, the relativistic Lippmann-Schwinger equation is introduced that is solved in order to obtain the $\Lambda_c^+\bar{\Lambda}_c^- \to \Lambda_c^+\bar{\Lambda}_c^-$ amplitude, and the equation for the distorted wave Born approximation that is used for calculating the amplitude for the $e^+e^- \to \Lambda_c^+\bar{\Lambda}_c^-$ transition. In Sec. III we describe our fitting procedure. The free parameters in the $\Lambda_c^+\bar{\Lambda}_c^-$ potential mentioned above are fixed in a fit to the cross-section data for $e^+e^- \to \Lambda_c^+\bar{\Lambda}_c^-$ by the Belle Collaboration [8]. An excellent reproduction of the experimental information can be achieved and is presented in Sec. III too. Furthermore, we extract the pole position of the $X(4630)$ that results from our fits and provide an estimate for the uncertainty. Finally, we summarize our results briefly in Sec. IV.

II. FORMALISM

The principal features of the formalism employed in the present study of the reaction $e^+e^- \to \Lambda_c^+\bar{\Lambda}_c^-$ are identical to the one developed and described in detail in Ref. [16] where the reaction $e^+e^- \to p\bar{p}$ was analyzed. Therefore, we will be very brief here and focus primarily on aspects where there are differences.

A. The $\Lambda_c^+\bar{\Lambda}_c^-$ interaction and the $e^+e^- \to \Lambda_c^+\bar{\Lambda}_c^-$ transition amplitude

The $N\bar{N}$ interaction as needed for a calculation of the timelike electromagnetic form factors of the proton near the $p\bar{p}$ threshold within the approach outlined in Ref. [16] is constrained by a wealth of empirical information from $p\bar{p} \to p\bar{p}$ and $p\bar{p} \to n\bar{n}$ scattering experiments. Specifically, there is a partial-wave analysis (PWA) available [18]. Indeed, in our investigation [16] we utilized a $N\bar{N}$ potential derived within chiral EFT [19], fitted to the results of the PWA. With

regard to the timelike electromagnetic form factors of the Λ the situation is somewhat different. Here the only constraints for the $\Lambda\bar{\Lambda}$ force are provided by FSI effects in the reaction $p\bar{p} \to \Lambda\bar{\Lambda}$. That reaction has been extensively investigated in the PS185 experiment at LEAR and data are available for total and differential cross sections but also for spin-dependent observables [20]. In our study of the reaction $e^+e^- \to \Lambda\bar{\Lambda}$ [17] we employed phenomenological $\Lambda\bar{\Lambda}$ potentials (based on meson-exchange) that were fitted to those PS185 data [21,22].

For the $\Lambda_c^+\bar{\Lambda}_c^-$ interaction there are no empirical constraints from hadronic reactions. In principle, one could follow the same strategy as done in Ref. [23] in an attempt to estimate the cross section for the reaction $p\bar{p} \to \Lambda_c^+\bar{\Lambda}_c^-$ and invoke SU(4) flavor symmetry to connect the $\Lambda_c^+\bar{\Lambda}_c^-$ interaction with the one in the $\Lambda\bar{\Lambda}$ system, see also Ref. [24]. However, in the present study we want to avoid to make any such basically phenomenological assumptions. Instead we aim at using the experimental information on the reaction $e^+e^- \to \Lambda_c^+\bar{\Lambda}_c^-$ itself to constrain and fix the interaction in the $\Lambda_c^+\bar{\Lambda}_c^-$ system. We will see and discuss below in how far this is possible.

In the actual construction of the $\Lambda_c^+\bar{\Lambda}_c^-$ interaction we adopt chiral EFT [25,26] as guide line and follow closely the procedure that has been already utilized in the derivation of our $N\bar{N}$ interaction [19,27]. In this framework the potential is given in terms of pion exchanges and a series of contact interactions with an increasing number of derivatives. The latter represent the short-range part of the baryon-baryon force and are parametrized by low-energy constants (LECs), that need to be fixed in a fit to data. Since we treat the reaction $e^+e^- \to \Lambda_c^+\bar{\Lambda}_c^-$ in the one-photon exchange approximation, the $\Lambda_c^+\bar{\Lambda}_c^-$ system can only be in the $^3S_1$ and $^3D_1$ partial waves. This limits rather strongly the number of LECs that need to be determined. Note also that there is no contribution from one-pion exchange because Λ_c^+ ($\bar{\Lambda}_c^-$) has isospin $I = 0$. Given that the energy region of interest is in the order of 100 MeV we restrict ourselves to interactions up to NLO in the chiral expansion. In principle, at NLO two-pion exchange contributions involving intermediate $\Sigma_c\bar{\Sigma}_c$ states arise. However, in view of the rather large mass difference $M_{\Sigma_c} - M_{\Lambda_c} \approx 167$ MeV we assume that such contributions can be effectively absorbed into the contact terms.

The explicit form of the contact terms up to NLO is, after partial-wave projection [27],

$$V(^3S_1)(p', p) = \tilde{C}_{^3S_1} + C_{^3S_1}(p'^2 + p^2)$$
$$- \mathrm{i}(\tilde{C}_{^3S_1}^a + C_{^3S_1}^a p'^2)(\tilde{C}_{^3S_1}^a + C_{^3S_1}^a p^2),$$

$$V(^3D_1 - {}^3S_1)(p', p) = C_{\epsilon_1} p'^2 - \mathrm{i}C_{\epsilon_1}^a p'^2(\tilde{C}_{^3S_1}^a + C_{^3S_1}^a p^2),$$

$$V(^3S_1 - {}^3D_1)(p', p) = C_{\epsilon_1} p^2 - \mathrm{i}(\tilde{C}_{^3S_1}^a + C_{^3S_1}^a p'^2)C_{\epsilon_1}^a p^2,$$

$$V(^3D_1)(p', p) = 0, \tag{1}$$

with $p = |\mathbf{p}|$ and $p' = |\mathbf{p}'|$ the initial and final center-of-mass momenta of the Λ_c^+ or $\bar{\Lambda}_c^-$. Here, the $\tilde{C}_i$ denote the LECs that arise at LO and that correspond to contact terms without derivatives, the C_i arise at NLO from contact terms with two derivatives. The term(s) right after the equality sign represent the elastic part of the $\Lambda_c^+ \bar{\Lambda}_c^-$ interaction. The annihilation part is described likewise by contact terms but with a somewhat different form, in analogy to the treatment of $N\bar{N}$ annihilation in our chiral EFT potential [19,27]. We refer the reader to Sec. 2.2 of Ref. [19] for a thorough discussion and justification for taking into account annihilation in this specific way. Here we just want to mention that the choice is dictated primarily by the requirement to manifestly fulfil unitarity constraints on a formal level. Note that in the expressions above the parameters $\tilde{C}^a$ and C^a are real quantities.

Since the Belle data suggest the presence of a resonance, the $X(4630)$ [8], we include also a resonance in the $\Lambda_c^+ \bar{\Lambda}_c^-$ potential. It is done in form of a pole diagram representing a bare vector-meson resonance with the quantum numbers $J^{PC} = 1^{--}$ and $I = 0$, corresponding to a ψ-type $c\bar{c}$ meson. Let us emphasize, however, that the introduction of such a pole diagram does not imply a bias for the dynamical origin of this resonance which is still controversially discussed in the literature [10–12,15]. We are here only concerned with the interplay of such a resonance structure (whatever its origin is) with the nonresonant part of the $\Lambda_c^+ \bar{\Lambda}_c^-$ interaction and its consequences for the shape and the actual position of the (physical) pole.

The potential is derived from the following Lagrangian that describes the coupling of a vector meson to the Λ_c ($\bar{\Lambda}_c$)

$$\mathcal{L} = g_V \bar{\Psi} \gamma^\mu \Psi \phi_\mu + \frac{f_V}{4M_{\Lambda_c}} \bar{\Psi} \sigma^{\mu\nu} \Psi (\partial_\mu \phi_\nu - \partial_\nu \phi_\mu) + \text{H.c.}, \quad (2)$$

with Ψ and ϕ representing the fields of the Λ_c^+ and the vector meson, respectively. The resulting potential after partial wave projection is of the form [28]

$$V_{^3S_1}(p', p; E) = \frac{4}{9m_V(E - m_V)} \left[g_V \left(1 + \frac{M_{\Lambda_c}}{2E_{p'}} \right) + f_V \left(\frac{E}{4M_{\Lambda_c}} + \frac{E}{2E_{p'}} \right) \right] \left[g_V \left(1 + \frac{M_{\Lambda_c}}{2E_p} \right) + f_V \left(\frac{E}{4M_{\Lambda_c}} + \frac{E}{2E_p} \right) \right],$$

$$V_{^3D_1}(p', p; E) = \frac{2}{9m_V(E - m_V)} \left[g_V \left(1 - \frac{M_{\Lambda_c}}{E_{p'}} \right) + f_V \left(\frac{E}{2E_{p'}} - \frac{E}{2M_{\Lambda_c}} \right) \right] \left[g_V \left(1 - \frac{M_{\Lambda_c}}{E_p} \right) + f_V \left(\frac{E}{2E_p} - \frac{E}{2M_{\Lambda_c}} \right) \right],$$

$$V_{^3D_1 - ^3S_1}(p', p; E) = \frac{2\sqrt{2}}{9m_V(E - m_V)} \left[g_V \left(1 - \frac{M_{\Lambda_c}}{E_{p'}} \right) + f_V \left(\frac{E}{2E_{p'}} - \frac{E}{2M_{\Lambda_c}} \right) \right] \left[g_V \left(1 + \frac{M_{\Lambda_c}}{2E_p} \right) + f_V \left(\frac{E}{4M_{\Lambda_c}} + \frac{E}{2E_p} \right) \right],$$

$$V_{^3S_1 - ^3D_1}(p', p; E) = \frac{2\sqrt{2}}{9m_V(E - m_V)} \left[g_V \left(1 + \frac{M_{\Lambda_c}}{2E_{p'}} \right) + f_V \left(\frac{E}{4M_{\Lambda_c}} + \frac{E}{2E_{p'}} \right) \right] \left[g_V \left(1 - \frac{M_{\Lambda_c}}{E_p} \right) + f_V \left(\frac{E}{2E_p} - \frac{E}{2M_{\Lambda_c}} \right) \right], \quad (3)$$

where $E_p = \sqrt{p^2 + M_{\Lambda_c}^2}$, $E_{p'} = \sqrt{p'^2 + M_{\Lambda_c}^2}$, and $E = \sqrt{s}$ is the total energy. The quantity m_V denotes the mass of the resonance, and g_V and f_V are the vector and tensor coupling constant, respectively. These are bare quantities and acquire their physical values by solving the Lippmann-Schwinger equation, see below.

The coupling between the $e^+ e^-$ and $\Lambda_c^+ \bar{\Lambda}_c^-$ systems is constructed in close analogy to our treatment of the photon coupling in pion photoproduction [29]. First we have a contact interaction, which actually corresponds to the situation considered in our studies of $e^+ e^- \to p\bar{p}$ and $e^+ e^- \to \Lambda\bar{\Lambda}$, and stands for a coupling via photon exchange. In addition, a direct coupling of the $e^+ e^-$ pair to $\Lambda_c^+ \bar{\Lambda}_c^-$ via the bare resonance is included. Thus, the Born amplitude for the transition $e^+ e^- \to \Lambda_c^+ \bar{\Lambda}_c^-$ is described by

$$F_{^3S_1}^0(p', p; E) = -\frac{4\alpha}{9} \left\{ G_{ee} \left(1 + \frac{M_{\Lambda_c}}{2E_{p'}} \right) + \frac{g_{ee}}{m_V(E - m_V)} \left[g_V \left(1 + \frac{M_{\Lambda_c}}{2E_{p'}} \right) + f_V \left(\frac{E}{4M_{\Lambda_c}} + \frac{E}{2E_{p'}} \right) \right] \right\} \left(1 + \frac{m_e}{2E_p} \right),$$

$$F_{^3D_1}^0(p', p; E) = -\frac{2\alpha}{9} \left\{ G_{ee} \left(1 - \frac{M_{\Lambda_c}}{E_{p'}} \right) + \frac{g_{ee}}{m_V(E - m_V)} \left[g_V \left(1 - \frac{M_{\Lambda_c}}{E_{p'}} \right) + f_V \left(\frac{E}{2E_{p'}} - \frac{E}{2M_{\Lambda_c}} \right) \right] \right\} \left(1 - \frac{m_e}{E_p} \right),$$

$$F_{^3D_1 - ^3S_1}^0(p', p; E) = -\frac{2\sqrt{2}\alpha}{9} \left\{ G_{ee} \left(1 - \frac{M_{\Lambda_c}}{E_{p'}} \right) + \frac{g_{ee}}{m_V(E - m_V)} \left[g_V \left(1 - \frac{M_{\Lambda_c}}{E_{p'}} \right) + f_V \left(\frac{E}{2E_{p'}} - \frac{E}{2M_{\Lambda_c}} \right) \right] \right\} \left(1 + \frac{m_e}{2E_p} \right),$$

$$F_{^3S_1 - ^3D_1}^0(p', p; E) = -\frac{2\sqrt{2}\alpha}{9} \left\{ G_{ee} \left(1 + \frac{M_{\Lambda_c}}{2E_{p'}} \right) + \frac{g_{ee}}{m_V(E - m_V)} \left[g_V \left(1 + \frac{M_{\Lambda_c}}{2E_{p'}} \right) + f_V \left(\frac{E}{4M_{\Lambda_c}} + \frac{E}{2E_{p'}} \right) \right] \right\} \left(1 - \frac{m_e}{E_p} \right). \quad (4)$$

The quantities G_{ee} and g_{ee} represent the strengths of the coupling via a contact term and the bare resonance, respectively. The notation is chosen in such a way that the nonpole contribution in Eq. (4) matches the one in the corresponding Eq. (6) of Ref. [16].

B. Scattering equation

The $\Lambda_c^+ \bar{\Lambda}_c^-$ amplitude is obtained from the solution of a relativistic Lippmann-Schwinger (LS) equation:

$$
\begin{aligned}
T_{L''L'}(p'', p'; E) = {} & V_{L''L'}(p'', p'; E) \\
& + \sum_L \int_0^\infty \frac{dp\, p^2}{(2\pi)^3} V_{L''L}(p'', p; E) \\
& \times \frac{1}{E - 2E_p + i0^+} T_{LL'}(p, p'; E),
\end{aligned} \quad (5)
$$

with $E = \sqrt{s}$. The potential V is the sum of contact terms, Eq. (1), and the pole diagram, Eq. (3). The scattering (on-shell) amplitude is given by $T_{L''L'}(k) := T_{L''L'}(k, k; E)$, with k the on-shell momentum defined by $E = 2E_k = 2\sqrt{M_{\Lambda_c}^2 + k^2}$. In our study of the reaction $e^+ e^- \to \Lambda_c^+ \bar{\Lambda}_c^-$ we restrict ourselves to the one-photon approximation [16] so that we need only the coupled partial waves ${}^3S_1$ and ${}^3D_1$, therefore L'', L', $L = 0, 2$. The amplitude for the reaction $e^+ e^- \to \Lambda_c^+ \bar{\Lambda}_c^-$ is evaluated in distorted wave Born approximation,

$$
\begin{aligned}
F_{L''L'}^{\Lambda_c^+ \bar{\Lambda}_c^-, e^+ e^-}(k, k_e; E) = {} & F_{L''L'}^0(k, k_e; E) \\
& + \sum_L \int_0^\infty \frac{dp\, p^2}{(2\pi)^3} T_{L''L}(k, p; E) \\
& \times \frac{1}{E - 2E_p + i0^+} F_{LL'}^0(p, k_e; E),
\end{aligned} \quad (6)
$$

with k_e the on-shell momentum of the $e^+ e^-$ pair and $E = 2E_k$. Here, $F_{L''L'}^0$ stands for the Born term for $e^+ e^- \to \Lambda_c^+ \bar{\Lambda}_c^-$ as given in Eq. (4). Like the $\Lambda_c^+ \bar{\Lambda}_c^-$ potential itself, it depends explicitly on the energy E because of the pole diagram, cf. Eq. (4). From the amplitude $F_{L''L'}^{\Lambda_c^+ \bar{\Lambda}_c^-, e^+ e^-}$ the $e^+ e^- \to \Lambda_c^+ \bar{\Lambda}_c^-$ cross section can be calculated in a straightforward way, but also any other observable of the reaction $e^+ e^- \to \Lambda_c^+ \bar{\Lambda}_c^-$, see Ref. [16].

The potential V that is inserted into the LS equation (5) needs to be regularized in order to suppress high-momentum components [25]. Following Refs. [26,27] we do this by introducing a regulator function with a cutoff mass. Since the contact interactions are nonlocal, cf. Eq. (1), a nonlocal regulator is applied. Its explicit form is [27]

$$
f(p', p) = \exp\left(-\frac{p'^m + p^m}{\Lambda^m}\right). \quad (7)
$$

In case of the transition potential for $e^+ e^- \to \Lambda_c^+ \bar{\Lambda}_c^-$ only the momentum in the $\Lambda_c^+ \bar{\Lambda}_c^-$ system acquires large values when evaluating Eq. (6) and, therefore, the corresponding contributions are likewise cut off. For the cutoff mass Λ we consider a range similar to the one regarded in Ref. [27]. Specifically, we employ values between 0.45 GeV and 0.85 GeV. Following [26], the exponent in the regulator is chosen to be $m = 2$.

We use the Λ_c^+ mass $M_{\Lambda_c} = 2286.46$ MeV [4] so that the $\Lambda_c^+ \bar{\Lambda}_c^-$ threshold is at $\sqrt{s} = 4572.92$ MeV. As in Ref. [16] we neglect the Coulomb interaction between the $\Lambda_c^+ \bar{\Lambda}_c^-$ when solving the LS equation but include its effect via the Sommerfeld-Gamow factor in the evaluation of the cross section. In general, we use the speed plot to determine the pole position. However, for the case of an elastic $\Lambda_c^+ \bar{\Lambda}_c^-$ interaction one can determine the pole also by an analytical continuation of the T matrix to the second Riemann sheet, by exploiting that zeros of the S-matrix on the first sheet correspond to poles on the second sheet. Doing so we can check the reliability of the results obtained from the speed plot.

III. RESULTS

A. Fitting procedure

The parameters of the $\Lambda_c^+ \bar{\Lambda}_c^-$ potential are determined in a fit to the $e^+ e^- \to \Lambda_c^+ \bar{\Lambda}_c^-$ cross section of the Belle Collaboration [8]. This concerns the LECs, see Eq. (1), but also the bare parameters of the resonance, m_V, g_V, and f_V. In the fit we consider data up to a kinetic center-of-mass energy of 100 MeV in the $\Lambda_c^+ \bar{\Lambda}_c^-$ system, which corresponds to $\sqrt{s} \leq 4.68$ GeV. Based on our experience with $e^+ e^- \to p\bar{p}$ and $e^+ e^- \to \Lambda\bar{\Lambda}$, we expect the (electromagnetic) couplings to the $e^+ e^-$ system (G_{ee}, g_{ee}) to be practically constant over that energy range so that they amount just to normalization factors.

With the above choice the data set comprises the first 6 points from Belle. However, since the point at the lowest energy is below the nominal $\Lambda_c^+ \bar{\Lambda}_c^-$ threshold it is not explicitly included in the least square minimization. Here we only make sure that our result at the threshold lies well within the pertinent bin. Note that the cross section for $e^+ e^- \to \Lambda_c^+ \bar{\Lambda}_c^-$ remains finite even at the $\Lambda_c^+ \bar{\Lambda}_c^-$ threshold because of the attractive Coulomb interaction between Λ_c^+ and $\bar{\Lambda}_c^-$, see the analogous situation for the $p\bar{p}$ final state [16].

For the analysis of the Belle data we consider a variety of fit scenarios. First of all, we explore in how far our results depend on the regularization procedure. For that we perform fits for a selection of cutoff masses between 0.45 and 0.85 GeV, so that we cover an even wider range as considered in the NN [26] and $N\bar{N}$ [27] studies. We perform also fits with a different number of contact terms in the $\Lambda_c^+ \bar{\Lambda}_c^-$ interaction, starting from a LO elastic $\Lambda_c^+ \bar{\Lambda}_c^-$
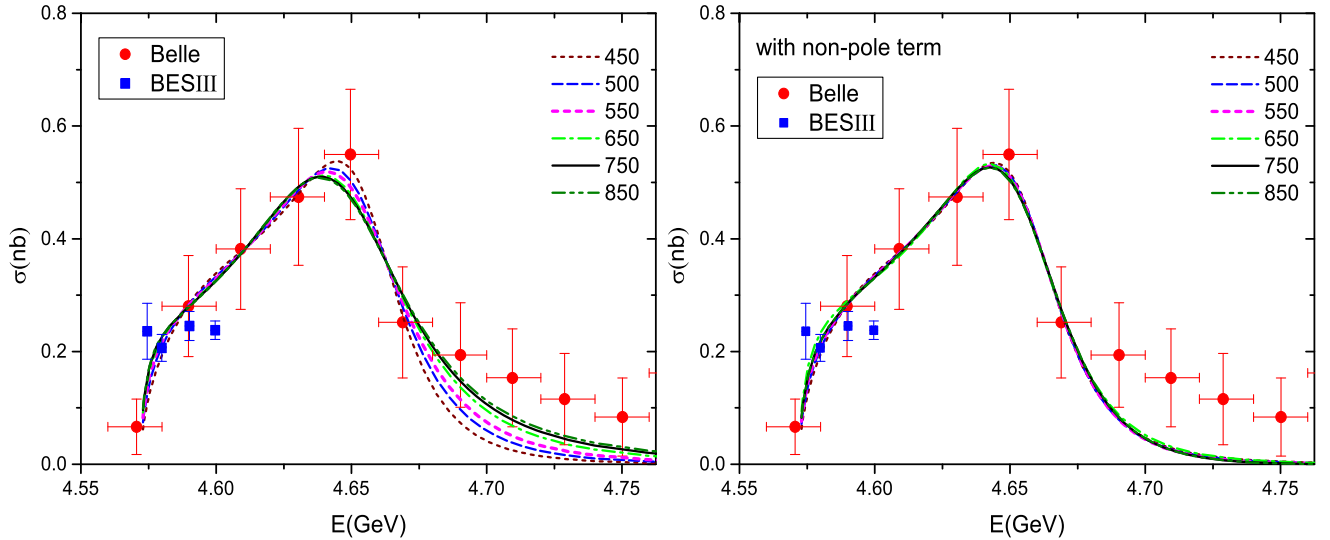
FIG. 1.   Fits to the $e^+e^- \to \Lambda_c^+ \bar{\Lambda}_c^-$ cross section of Belle [8] (red circles) for various cutoff masses Λ at LO and without annihilation. Left: Coupling between e^+e^- and $\Lambda_c^+ \bar{\Lambda}_c^-$ only via pole term. Right: Coupling between e^+e^- and $\Lambda_c^+ \bar{\Lambda}_c^-$ via pole term plus nonpole term, cf. Eq. (4). The data from BESIII [30] (blue squares) are included for illustration.

potential (one contact term, $\tilde{C}_{^3S_1}$) up to NLO and including an elastic part as well as annihilation (four contact terms, $\tilde{C}_{^3S_1}$, $\tilde{C}_{^3S_1}^a$, $C_{^3S_1}$, $C_{^3S_1}^a$). Finally, we consider the cases where the e^+e^- state couples to the $\Lambda_c^+ \bar{\Lambda}_c^-$ system only via the resonance and where it couples also directly via the photon, which corresponds to a contact interaction in our formalism.

In exploratory fits we included also the contact terms C_{ε_1}, $C_{\varepsilon_1}^a$ that introduce a $^3S_1$-$^3D_1$ coupling. However, it turned out that the Belle data [8] do not allow one to fix those terms and results with or without them were practically indistinguishable. Thus, we set them to zero. The same is also the case with the tensor coupling constant f_V of the pole diagram, cf. Eq. (3), so that we put $f_V = 0$ in our analysis.

In a first series of fits we included only the contact term $\tilde{C}_{^3S_1}$, corresponding to a purely elastic $\Lambda_c^+ \bar{\Lambda}_c^-$ potential at LO, together with the pole diagram and varied the cutoff mass Λ. The resulting cross sections are displayed in Fig. 1 for the cases where the e^+e^- system couples either only via the resonance to $\Lambda_c^+ \bar{\Lambda}_c^-$ (left side) or also via a contact term (right side). The numerical values of the parameters are compiled in Table I. In a second series of fits we added more and more terms in the contact interaction, allowing not only for elastic scattering but also for annihilation in the $\Lambda_c^+ \bar{\Lambda}_c^-$ channel. Here the cutoff mass is kept the same for all interactions and fixed to $\Lambda = 0.75$ GeV. The resulting cross sections are displayed in Fig. 2, again for the cases where the e^+e^- system couples either only via the resonance to $\Lambda_c^+ \bar{\Lambda}_c^-$ (left side) or also via a contact term (right side). The numerical values of the parameters are compiled in Table II.

B. Discussion of results

The results presented in Figs. 1 and 2 attest that the Belle data can be reproduced rather well over the fitting range within all scenarios considered. Differences in the cross sections appear mainly at higher energies. There is also some variation around the maximum, where the fits that include a non-pole term in the electromagnetic coupling reproduce the peak value and the subsequent sharp drop in the cross section visibly better. Note that in the course of our study we have also performed extended fits where all data points up to 4.75 GeV were included (though by giving less weight to the data at higher energies). Those led to results that are practically identical to the ones shown in Figs. 1 and 2.

Let us discuss the results more thoroughly and, to begin with, look at the cutoff dependence. There are still noticeable variations in the scenario where only the coupling via a pole term is considered (upper part of Table I). Specifically, there is an observable deterioration in the achieved χ^2 with increasing cutoff mass. Moreover, there is a pronounced variation of the $\Lambda_c^+ \bar{\Lambda}_c^-$ $^3S_1$ scattering length a. On the other hand, the resonance parameters themselves are less sensitive to the cutoff. The variations of the resonance parameters, given in terms of the real and imaginary part of the pole position in Table I, are in the order of 10 MeV or so. Evidently, once a nonpole contribution is added the cutoff dependence is remarkably reduced, cf. the lower part of Table I. First, now the achieved χ^2 is practically the same for all cutoffs. The variation in a is much smaller and, actually, within the expected uncertainty for the determination of the scattering length from an FSI analysis estimated in Ref. [31] on general grounds. Finally, the variation in the resonance mass is only about 2 MeV, and

TABLE I.   Parameters of the fit at LO and without annihilation, for different cutoff masses Λ. The given χ^2 is for the data points below $\sqrt{s} = 4.68$ GeV, see text. The $\Lambda_c^+ \bar{\Lambda}_c^-$ scattering length in the $^3S_1$ partial wave is denoted by a.

Λ (GeV)	0.45	0.50	0.55	0.65	0.75	0.85
with pole term, see Eq. (4)						
$\tilde{C}_{^3S_1}$ (GeV^{-2})	191.8	110.1	61.27	7.853	−19.17	−34.48
g_V	−8.734	−8.123	−7.625	−6.837	−6.218	−5.706
m_V (GeV)	4.6344	4.6364	4.6383	4.6419	4.6448	4.6472
$g_{ee}(\times10^{-3}$ GeV$^2)$	1.052	1.067	1.081	1.102	1.116	1.126
χ^2	0.1	0.3	0.4	0.6	0.7	0.8
pole (GeV)	4.6550 − i0.0264	4.6534 − i0.0311	4.6514 − i0.0343	4.6482 − i0.0376	4.6462 − i0.0389	4.6451 − i0.0394
a (fm)	−0.269	−0.485	−0.634	−0.818	−0.927	−1.002
with pole and nonpole contribution, see Eq. (4)						
$\tilde{C}_{^3S_1}$ (GeV^{-2})	191.9	111.9	65.65	−0.0100	−11.76	−26.96
g_V	−8.808	−7.964	−7.356	−6.490	−5.899	−5.415
m_V (GeV)	4.6328	4.6398	4.6443	4.6473	4.6542	4.6572
$g_{ee}(\times10^{-3}$ GeV$^2)$	1.055	1.052	1.042	1.045	1.004	0.987
$G_{ee}(\times10^{-3})$	0.272	−0.578	−1.035	−1.100	−1.672	−1.787
χ^2	0.1	0.1	0.2	0.2	0.2	0.2
pole (GeV)	4.6543 − i0.0276	4.6552 − i0.0284	4.6554 − i0.0295	4.6532 − i0.0304	4.6550 − i0.0314	4.6549 − i0.0319
a (fm)	−0.325	−0.360	−0.403	−0.641	−0.538	−0.581

around 8 MeV for the width. We interpret these variations as the inherent systematic error of our analysis.

Results considering variations of the $\Lambda_c^+ \bar{\Lambda}_c^-$ interaction are summarized in Table II. Since the influence of the cutoff has been established above, we show only results for a fixed cutoff value, namely for $\Lambda = 0.75$ GeV. Again, fits that include either a pole term alone or a pole and a nonpole coupling to e^+e^- have been performed. However, in view of the preceding discussion we expect primarily the latter

scenario to provide reliable and physically meaningful results. Indeed, again practically the same χ^2 could be achieved, independently of whether just a single term (elastic) $\Lambda_c^+ \bar{\Lambda}_c^-$ interaction is employed or one with 4 LECs that involves contributions to the elastic part and annihilation up to NLO. Actually, now also the resulting scattering lengths are fairly close together, at least for the first three $\Lambda_c^+ \bar{\Lambda}_c^-$ potentials. Only for the one with 4 LECs there is a striking difference. It has to be said, however, that
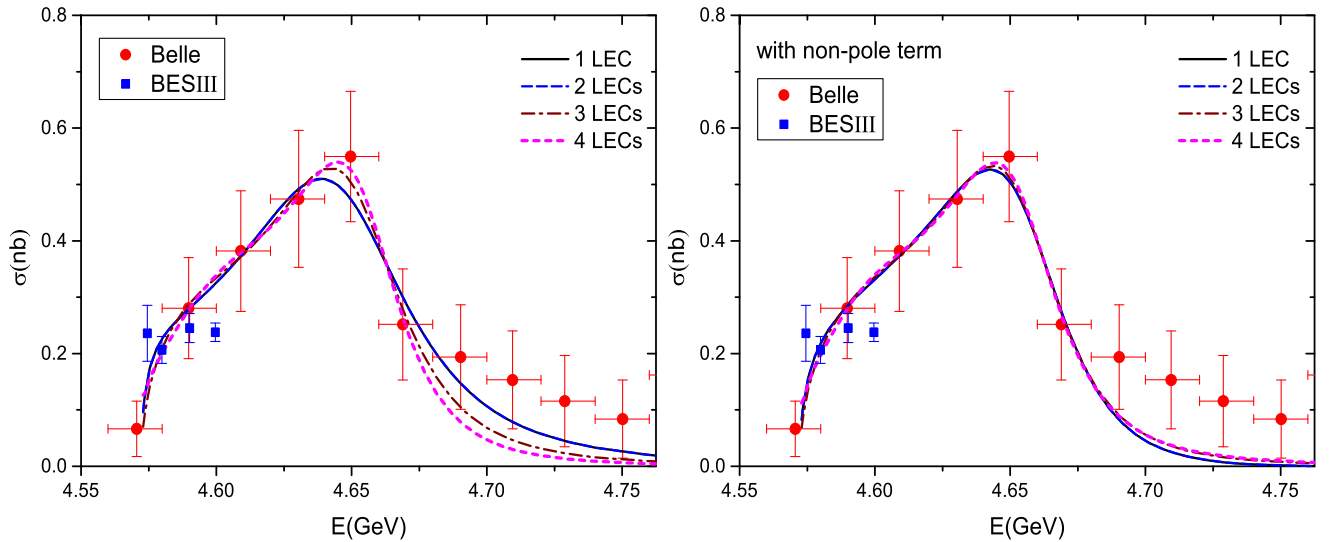

FIG. 2.   Fits to the $e^+e^- \to \Lambda_c^+ \bar{\Lambda}_c^-$ cross section of Belle [8] (red circles) at LO, without (1 LEC) and with annihilation term (2 LECs), and up to NLO, without (3 LECs) and with annihilation term (4 LECs). Left: Coupling between e^+e^- and $\Lambda_c^+ \bar{\Lambda}_c^-$ only via pole term. Right: Coupling between e^+e^- and $\Lambda_c^+ \bar{\Lambda}_c^-$ via pole term plus nonpole term, cf. Eq. (4). The data from BESIII [30] (blue squares) are included for illustration.

TABLE II.   Parameters of the fits up to NLO, with/without annihilation term. The cutoff mass Λ is 0.75 GeV. The given χ^2 is for the data points below $\sqrt{s} = 4.68$ GeV, see text. The $\Lambda_c^+ \bar{\Lambda}_c^-$ scattering length in the $^3S_1$ partial wave is denoted by a.

	1 LEC	2 LECs	3 LECs	4 LECs
with pole term, see Eq. (4)				
$\tilde{C}_{^3S_1}$ (GeV^{-2})	-19.17	-19.23	-0.1001	-49.78
$C_{^3S_1}$ (GeV^{-4})	$\cdots$	$\cdots$	-191.3	-146.4
$\tilde{C}^a_{^3S_1}$ (GeV^{-1})	$\cdots$	0.1661	-0.5353	-1159
$C^a_{^3S_1}$ (GeV^{-3})	$\cdots$	$\cdots$	$\cdots$	4567
g_V	-6.218	-6.218	-5.071	-4.705
m_V (GeV)	4.6448	4.6448	4.6386	4.6362
$g_{ee}(\times 10^{-3}$ GeV^2)	1.116	1.116	1.079	1.171
χ^2	0.7	0.7	0.3	0.1
pole (GeV)	$4.6462 - i0.0389$	$4.6455 - i0.0390$	$4.6501 - i0.0396$	$4.6506 - i0.0397$
a (fm)	-0.927	-0.928	-0.726	$-0.916 - i0.844$

	1 LEC	2 LECs	3 LECs	4 LECs
with pole and nonpole contribution, see Eq. (4)				
$\tilde{C}_{^3S_1}$ (GeV^{-2})	-11.76	$-11.74)$	-0.0135	-60.76
$C_{^3S_1}$ (GeV^{-4})	$\cdots$	$\cdots$	-187.9	-74.23
$\tilde{C}^a_{^3S_1}$ (GeV^{-1})	$\cdots$	0.6595	0.0503	-1185
$C^a_{^3S_1}$ (GeV^{-3})	$\cdots$	$\cdots$	$\cdots$	5455
g_V	-5.899	-5.897	-5.012	-4.858
m_V (GeV)	4.6542	4.6542	4.6414	4.6342
$g_{ee}(\times 10^{-3}$ GeV^2)	1.004	1.003	1.063	1.200
$G_{ee}(\times 10^{-3})$	-1.672	-1.679	-0.455	0.512
χ^2	0.2	0.2	0.2	0.1
pole (GeV)	$4.6550 - i0.0314$	$4.6546 - i0.0312$	$4.6520 - i0.0285$	$4.6482 - i0.0341$
a (fm)	-0.538	-0.537	-0.632	$-0.981 - i0.714$

in this particular fit we have tried intentionally to increase annihilation as much as possible—in order to explore possible consequences for the resulting scattering length but also the pole position. As such, this exercise reveals that the $e^+ e^- \to \Lambda_c^+ \bar{\Lambda}_c^-$ cross-section data do not allow a unique determination of the $\Lambda_c^+ \bar{\Lambda}_c^-$ interaction. However, in view of the presence of annihilation in the $\Lambda_c^+ \bar{\Lambda}_c^-$ channel this is not really a surprise.

Fortunately, the resonance parameters are much less sensitive to details of the $\Lambda_c^+ \bar{\Lambda}_c^-$ interaction and, specifically, to the strength of annihilation, cf. the corresponding results in the lower part of Table II. Utilizing these variations as basis for estimating the uncertainty of the resonance parameters of the $X(4630)$ we arrive at $M = (4652.5 \pm 3.4)$ MeV and $\Gamma = (62.6 \pm 5.6)$ MeV. These values have to be compared with the ones from the Belle fit which are $M = 4634^{+8}_{-7}{}^{+5}_{-8}$ MeV and $\Gamma = 92^{+40}_{-24}{}^{+10}_{-21}$ MeV [8]. Though our results agree with the ones of Belle within the given uncertainties, the central value of the resonance mass extracted from our analysis is clearly shifted upwards by about 20 MeV as compared to the one from the Breit-Wigner fit, while the width is significantly smaller. The latest results for the $X(4660)$

from measurements of the $\pi^+ \pi^- \psi(2S)$ channel are $M = (4652 \pm 10 \pm 8)$ MeV   and $\Gamma = (68 \pm 11 \pm 1)$ MeV (Belle [7]), and $M = (4669 \pm 21 \pm 3)$ MeV and $\Gamma = (104 \pm 48 \pm 10)$ MeV (BABAR [6]). Obviously, there is a remarkable agreement between our $X(4630)$ parameters determined from $e^+ e^- \to \Lambda_c^+ \bar{\Lambda}_c^-$ data with the ones extracted by Belle for the $X(4660)$ in the $e^+ e^- \to \pi^+ \pi^- \psi(2S)$ decay. The $X(4660)$ parameters given by BABAR are somewhat different, but one has to take into consideration that the uncertainties are much larger in the latter determination. An overview of the resonance parameters is provided in Table III.

We do not include the $\Lambda_c^+ \bar{\Lambda}_c^-$ invariant mass spectrum measured in the reaction $\bar{B} \to \Lambda_c^+ \bar{\Lambda}_c^- \bar{K}$ [9] in our fit. Given that $M_B = 5279$ MeV and $2M_{\Lambda_c} + M_K \approx 4948$ MeV the phase space for the decay $\bar{B} \to \Lambda_c^+ \bar{\Lambda}_c^- \bar{K}$ is fairly small. Because of that it is likely that the $\Lambda_c^+ \bar{\Lambda}_c^-$ spectrum is significantly distorted by possible interactions in the other subsystems, $\Lambda_c^+ K^-$ and/or $\bar{\Lambda}_c^- K^-$. Indeed, the invariant mass spectrum for $\Lambda_c^+ K^-$ shown in Ref. [9] suggests the presence of a Ξ_c resonance in that channel around 2930 MeV. See also the related discussion in Ref. [14]. Further complications for an analysis are the relatively low

TABLE III.   Overview of resonance parameters for the $X(4630)$ and $X(4660)$, respectively.

	present analysis	Belle [8]	Belle [7]	BABAR [6]
reaction	$e^+e^- \to \Lambda_c^+ \bar{\Lambda}_c^-$	$e^+e^- \to \Lambda_c^+ \bar{\Lambda}_c^-$	$e^+e^- \to \pi^+\pi^-\psi(2S)$	$e^+e^- \to \pi^+\pi^-\psi(2S)$
mass M (MeV)	$4652.5 \pm 3.4 \pm 1.1$	$4634^{+8\ +5}_{-7\ -8}$	$4652 \pm 10 \pm 8$	$4669 \pm 21 \pm 3$
width Γ (MeV)	$62.6 \pm 5.6 \pm 4.3$	$92^{+40\ +10}_{-24\ -21}$	$68 \pm 11 \pm 1$	$104 \pm 48 \pm 10$

statistics of the data and the fact that $\Lambda_c^+ \bar{\Lambda}_c^-$ FSI effects could come not only from the $^3S_1$ but also from the $^1S_0$ partial wave, because parity is not conserved in this decay so that the $\bar{K}$ can be in an s- or p wave.

C. Outlook on the Λ_c electromagnetic form factors

One of the motivations for measurements of reactions like $e^+e^- \to p\bar{p}$ and $e^+e^- \to \Lambda\bar{\Lambda}$ is that one can determine the electromagnetic form factors of the corresponding baryons in the timelike region [32]. This applies also to the Λ_c^+. Indeed, recently a new measurement of the reaction $e^+e^- \to \Lambda_c^+ \bar{\Lambda}_c^-$ has been performed by the BESIII Collaboration [30] and first results for the ratio of the Λ_c^+ electromagnetic form factors G_E and G_M have been presented.

We include the cross section data from the BESIII measurement in Figs. 1 and 2 for illustration. However, we want to emphasize that they were not taken into account in our analysis of the $X(4630)$, which is the main goal of the present paper. While these data agree with the ones from the Belle Collaboration [8] as far as the magnitude of the reaction cross section is concerned, they seem to indicate a different trend for the energy dependence. Exploratory fits with inclusion of those data revealed that it is practically impossible to reconcile this trend with the Belle data at

energies around the $X(4630)$ peak based on a $\Lambda_c^+ \bar{\Lambda}_c^-$ FSI that is constructed along the lines of chiral EFT, see Eqs. (1) and (3). Hopefully, the BESIII Collaboration will be able to extend their measurements to somewhat higher energies and, thereby, clarify the situation. If the trend suggested by the BESIII data (cf. Figs. 1 and 2) persists even for energies closer to the $X(4630)$, it will have a drastic impact on the actual parameters of the resonance. Anyway, in anticipation of future results from BESIII, predictions for the effective electromagnetic form factor of the Λ_c (G_{eff}) are displayed in Fig. 3, for the fits where the e^+e^- pair couples to $\Lambda_c^+ \bar{\Lambda}_c^-$ via the pole term alone. Results for the variants where a nonpole coupling is included are very similar and, therefore, not shown. For the definition of G_{eff} see, e.g., Ref. [16].

There are also results for the angular distribution of the Λ_c in Ref. [30]. The data are for $\sqrt{s} = 4.5745$ GeV and $\sqrt{s} = 4.5995$ GeV, respectively, corresponding to kinetic energies of 1.6 MeV and 26.6 MeV in the $\Lambda_c^+ \bar{\Lambda}_c^-$ system. At the lower energy the angular distribution is rather flat suggesting that the $\Lambda_c^+ \bar{\Lambda}_c^-$ state is produced almost entirely in the $^3S_1$ partial wave. This behavior is well in line with our calculation. At the higher energy the data indicate the presence of contributions from the $^3D_1$ partial wave. Thus, in a future analysis one could use those data to fix the
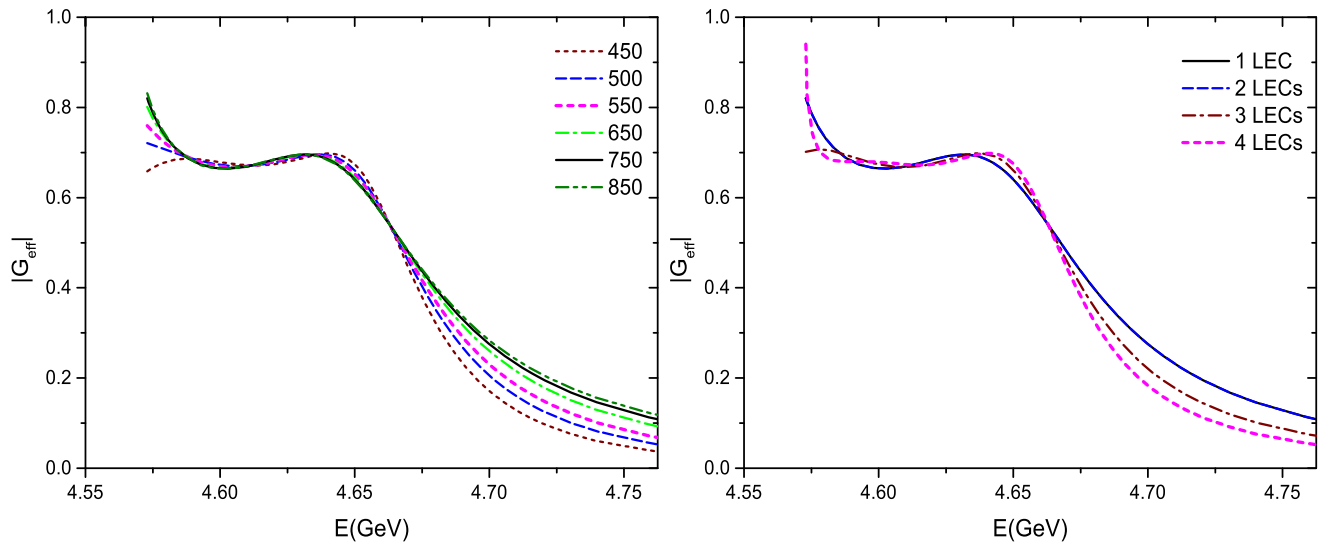

FIG. 3.   Prediction for the effective form factor G_{eff}. Left panel: LO results for various values of the cutoff Λ. Right panel: Results at LO and NLO, with/without annihilation term. The cutoff mass Λ is 0.75 GeV. For a detailed description of the employed $\Lambda_c^+ \bar{\Lambda}_c^-$ interactions, see text.

additional LECs (C_{ε_1}, $C^a_{\varepsilon_1}$) in our NLO interaction, see Eq. (1), which could not be determined from the Belle data, as discussed in Sec. III. A. Also here results at higher energies would be rather helpful in order to map out the actual energy dependence of the D-wave contribution.

IV. SUMMARY

In the present work we investigated the reaction $e^+e^- \to \Lambda^+_c \bar{\Lambda}^-_c$ at energies close to the threshold with the aim to examine the impact of the $X(4630)$ resonance and to determine its parameters. Thereby, special emphasis was put on a rigorous treatment of the interaction in the final $\Lambda^+_c \bar{\Lambda}^-_c$ state. The latter was done in distorted wave Born approximation, following our works on $e^+e^- \to p\bar{p}$ [16] and $e^+e^- \to \Lambda\bar{\Lambda}$ [17].

The relevant interaction in the $\Lambda^+_c \bar{\Lambda}^-_c$ system was constructed along the lines of chiral effective field theory up to next-to-leading order, supplemented by a pole diagram that represents a bare $X(4630)$ resonance. The inherent parameters (low-energy constants, bare mass and coupling constant of the resonance) were determined in a fit to the $e^+e^- \to \Lambda^+_c \bar{\Lambda}^-_c$ data of the Belle Collaboration [8]. Since it turned out that a unique determination of involved parameters in a fit to these data is not possible we considered a variety of scenarios in order to estimate the uncertainty of the results for the $X(4630)$ resonance. Based on those variants the pole parameters of the $X(4630)$ were found to be $M = (4652.5 \pm 3.4 \pm 1.1)$ MeV and $\Gamma = (62.6 \pm 5.6 \pm 4.3)$ MeV, where the first uncertainty is due to variations in the $\Lambda^+_c \bar{\Lambda}^-_c$ interaction and the second value reflects the uncertainty due to the employed regularization scheme.

Our values are remarkably close to the ones of the $X(4660)$ resonance that have been established in the reaction $e^+e^- \to \pi^+\pi^-\psi(2S)$ [6,7]. Therefore, we confirm a conjecture that has been already put forward shortly after the $e^+e^- \to \Lambda^+_c \bar{\Lambda}^-_c$ data were published, namely that the $X(4630)$ and $X(4660)$ resonances could be the same states [10–12]. We want to emphasize, however, that the present work takes into account the rather delicate interplay between the resonance and a possible residual interaction in the $\Lambda^+_c \bar{\Lambda}^-_c$ system for the first time in a compelling way. Because of that we consider the outcome of the present analysis to be more conclusive. In particular, results could be achieved that are reliable on a quantitative level.

Finally, since new measurements for the reaction $e^+e^- \to \Lambda^+_c \bar{\Lambda}^-_c$ are presently performed by the BESIII Collaboration, with higher statistics and better energy resolution [30], we presented also predictions for the Λ_c electromagnetic form factors in the timelike region. Indeed, our approach is well suited to perform also calculations (and an analysis) of other and more subtle observables of the reaction $e^+e^- \to \Lambda^+_c \bar{\Lambda}^-_c$ such as angular distributions, polarizations, or spin-correlation parameters, once they become available [33].

[1] F.-K. Guo, C. Hanhart, U.-G. Meißner, Q. Wang, Q. Zhao, and B.-S. Zou, Hadronic molecules, arXiv:1705.00141 [Rev. Mod. Phys. (to be published)].

[2] H.-X. Chen, W. Chen, X. Liu, Y.-R. Liu, and S.-L. Zhu, A review of the open charm and open bottom systems, Rep. Prog. Phys. **80**, 076201 (2017).

[3] A. Esposito, A. Pilloni, and A. D. Polosa, Multiquark resonances, Phys. Rep. **668**, 1 (2017).

[4] C. Patrignani et al. (PDG Collaboration), Review of particle physics, Chin. Phys. C **40**, 100001 (2016).

[5] X. L. Wang et al. (Belle Collaboration), Observation of Two Resonant Structures in $e^+e^- \to \pi^+\pi^-\psi(2S)$ via Initial State Radiation at Belle, Phys. Rev. Lett. **99**, 142002 (2007).

[6] J. P. Lees et al. (BABAR Collaboration), Study of the reaction $e^+e^- \to \psi(2S)\pi^-\pi^-$ via initial-state radiation at BABAR, Phys. Rev. D **89**, 111103 (2014).

[7] X. L. Wang et al. (Belle Collaboration), Measurement of $e^+e^- \to \pi^+\pi^-\psi(2S)$ via Initial State Radiation at Belle, Phys. Rev. D **91**, 112007 (2015).

[8] G. Pakhlova et al. (Belle Collaboration), Observation of a Near-Threshold Enhancement in the $e^+e^- \to \Lambda^+_c \bar{\Lambda}^-_c$ Cross Section Using Initial-State Radiation Phys. Rev. Lett. **101**, 172001 (2008).

[9] B. Aubert et al. (BABAR Collaboration), Study of $\bar{B} \to \Xi_c \bar{\Delta}_c^-$ and $\bar{B} \to \Lambda^+_c \bar{\Lambda}^-_c \bar{K}$ decays at BABAR, Phys. Rev. D **77**, 031101 (2008).

[10] D. V. Bugg, An alternative fit to Belle mass spectra for $D\bar{D}$, $D^*\bar{D}^*$ and $\Lambda_c\bar{\Lambda}_c$, J. Phys. G **36**, 075002 (2009).

[11] G. Cotugno, R. Faccini, A. D. Polosa, and C. Sabelli, Charmed Baryonium, Phys. Rev. Lett. **104**, 132005 (2010).

[12] F. K. Guo, J. Haidenbauer, C. Hanhart, and U.-G. Meißner, Reconciling the $X(4630)$ with the $Y(4660)$, Phys. Rev. D **82**, 094008 (2010).

[13] B. Q. Li and K. T. Chao, Higher charmonia and X,Y,Z states with screened potential, Phys. Rev. D **79**, 094004 (2009).

[14] F. K. Guo, C. Hanhart, and U.-G. Meißner, Evidence that the $Y(4660)$ is a f(0)(980) psi-prime bound state, Phys. Lett. B **665**, 26 (2008).

[15] E. van Beveren, X. Liu, R. Coimbra, and G. Rupp, Possible $\Psi(5S)$, $\Psi(4D)$, $\Psi(6S)$ and $\Psi(5D)$ signals in $\Lambda\bar{\Lambda}$, Europhys. Lett. **85**, 61002 (2009).

[16] J. Haidenbauer, X.-W. Kang, and U.-G. Meißner, The electromagnetic form factors of the proton in the timelike region, Nucl. Phys. **A929**, 102 (2014).

[17] J. Haidenbauer and U.-G. Meißner, The electromagnetic form factors of the Λ in the timelike region, Phys. Lett. B **761**, 456 (2016).

[18] D. Zhou and R. G. E. Timmermans, Energy-dependent partial-wave analysis of all antiproton-proton scattering data below 925 MeV/c, Phys. Rev. C **86**, 044003 (2012).

[19] X. W. Kang, J. Haidenbauer, and U.-G. Meißner, Antinucleon-nucleon interaction in chiral effective field theory, J. High Energy Phys. 02 (2014) 113.

[20] E. Klempt, F. Bradamante, A. Martin, and J.-M. Richard, Antinucleon–nucleon interaction at low energy: scattering and protonium, Phys. Rep. **368**, 119 (2002).

[21] J. Haidenbauer, T. Hippchen, K. Holinde, B. Holzenkamp, V. Mull, and J. Speth, The reaction $\bar{p}p \to \bar{\Lambda}\Lambda$ in the meson exchange picture, Phys. Rev. C **45**, 931 (1992).

[22] J. Haidenbauer, K. Holinde, V. Mull, and J. Speth, Meson exchange and quark-gluon transitions in the $\bar{p}p \to \bar{\Lambda}\Lambda$ process, Phys. Rev. C **46**, 2158 (1992).

[23] J. Haidenbauer and G. Krein, The reaction $\bar{p}p \to \bar{\Lambda}_c^-\Lambda_c^+$ close to threshold, Phys. Lett. B **687**, 314 (2010).

[24] Y.-Y. Wang, Q.-F. Lü, E. Wang, and D.-M. Li, Role of $Y(4630)$ in the $p\bar{p} \to \Lambda_c\bar{\Lambda}_c$ reaction near threshold, Phys. Rev. D **94**, 014025 (2016).

[25] E. Epelbaum, H.-W. Hammer, and U.-G. Meißner, Modern theory of nuclear forces, Rev. Mod. Phys. **81**, 1773 (2009).

[26] E. Epelbaum, H. Krebs, and U.-G. Meißner, Improved chiral nucleon-nucleon potential up to next-to-next-to-next-to-leading order, Eur. Phys. J. A **51**, 53 (2015).

[27] L. Y. Dai, J. Haidenbauer, and U.-G. Meißner, Antinucleon-nucleon interaction at next-to-next-to-next-to-leading order in chiral effective field theory, J. High Energy Phys. 07 (2017) 078.

[28] T. Hippchen, PhD thesis, Jül-Spez-494 Forschungszentrum Jülich GmbH, 1989.

[29] D. Rönchen, M. Döring, F. Huang, H. Haberzettl, J. Haidenbauer, C. Hanhart, S. Krewald, U.-G. Meißner, and K. Nakayama, Photocouplings at the pole from pion photoproduction, Eur. Phys. J. A **50**, 101 (2014).

[30] M. Ablikim et al., Precision measurement of the $e^+e^- \to \Lambda_c^+\bar{\Lambda}_c^-$ cross section near threshold, arXiv:1710.00150.

[31] A. Gasparyan, J. Haidenbauer, C. Hanhart, and J. Speth, How to extract the ΛN scattering length from production reactions, Phys. Rev. C **69**, 034006 (2004).

[32] A. Denig and G. Salmè, Nucleon electromagnetic form factors in the timelike region, Prog. Part. Nucl. Phys. **68**, 113 (2013).

[33] C. Morales Morales (BESIII Collaboration), Baryon Electromagnetic Form Factors at BESIII, arXiv:1706.07674.